Optik - International Journal for Light and Electron Optics 195 (2019) 163157

Contents lists available at ScienceDirect

Optik

journal homepage: www.elsevier.com/locate/ijleo

Holmium based nanoseconds pulsed fibre laser generation in the 2-micron region

M.F.A. Rahman[a,b], M.B.H. Mahyuddin[a], A.A. Latiff[c], M.C. Paul[d], A. Dhar[d], S. Das[d], P. Yupapin[e,f], M. Yasin[g,*], S.W. Harun[a,*]

[a] Photonics Engineering Laboratory, Department of Electrical Engineering, Faculty of Engineering, University of Malaya, 50603 Kuala Lumpur, Malaysia
[b] Faculty of Engineering Technology, Universiti Teknikal Malaysia Melaka, 76100 Hang Tuah Jaya, Melaka, Malaysia
[c] Fakulti Teknologi Kejuruteraan Elektrik & Elektronik, Universiti Teknikal Malaysia Melaka, 76100 Hang Tuah Jaya, Melaka, Malaysia
[d] Fiber Optics and Photonics Division, CSIR-Central Glass and Ceramic Research Institute, 196, Raja S.C. Mullick Road, Kolkata, 700032, India
[e] Computational Optics Research Group, Advanced Institute of Materials Science, Ton Duc Thang University, District 7, Ho Chi Minh City, 700000, Viet Nam
[f] Faculty of Applied Sciences, Ton Duc Thang University, District 7, Ho Chi Minh City, 700000, Viet Nam
[g] Department of Physics, Faculty of Science and Technology, Airlangga University, Surabaya, Indonesia

ARTICLE INFO

Keywords:
Optical fibre laser
Fibre saturable absorber
Holmium
Thin film

ABSTRACT

We demonstrate and compare nanoseconds pulse induced by a Holmium oxide PVA film (HOPF, 50 μm thick) and a Holmium-doped fibre (HDF, 8 cm long) saturable absorber (SA) in a Thulium doped-fibre laser (TDFL) cavity. The HOPF SA produced a nanoseconds pulse operating at 1960 nm wavelength, with a pulse width of 57 ns. On the other hand, the HDF SA produced a pulsed laser operating at 1963 nm wavelength, with a pulse width of 53 ns. The HDF SA established a slightly better maximum pulse energy of 0.87 nJ as compared to the HOPF SA with only 0.62 nJ.

1. Introduction

In recent years, passive saturable absorbers (SAs) have received tremendous attention particularly in the generation of stable short-pulsed fibre lasers in the 2-micron region. These pulsed-lasers feature eye-safe, wide tunable bandwidth, and high-water absorbent. Apart from that, they are also suitable for various laser applications, including medical surgery [1,2], polymer welding [3], gas sensing, Light detection and ranging (LIDAR), and free-space telecommunication. However, the recent inventions are seemed to be focusing more on the high peak power mode-locked picoseconds or femtoseconds pulsed fibre lasers [4–6], leaving nanoseconds pulsed fibre laser slightly left behind.

Typically, nanoseconds pulsed-fibre lasers generate much lower peak power and much greater pulse energy. In an early report, a nanoseconds pulse was demonstrated by using a nanotube-polymer film SA in a Ytterbium-doped fibre laser (YDFL) cavity [7]. An additional cavity length was employed in the resonator to increase the pulse energy and the pulse width, causing the peak power to reduce. Xia et al. demonstrated a nanoseconds pulse in an Erbium-doped fibre laser (EDFL) by incorporating a monolayer graphene film SA [8]. A supplementary long fibre consisting of normal dispersion and nonlinearity effect was utilized in the set-up. The employment of this extra fibre caused the pulse to broaden up to 24 ns, while at the same time increasing its pulse energy, and

* Corresponding authors.
E-mail addresses: yasin@fst.unair.ac.id (M. Yasin), swharun@um.edu.my (S.W. Harun).

https://doi.org/10.1016/j.ijleo.2019.163157
Received 16 June 2019; Received in revised form 19 July 2019; Accepted 24 July 2019

decreasing its peak power. In another report, a Molybdenum disulfide (MoS_2) SA was employed into a YDFL cavity for nanoseconds pulse generation [9]. The cavity had a total length of 92 m and was believed to be dominated by an additional long single-mode fibre (SMF) integrated into the cavity. Overall, these pulsed fibre lasers with low peak power and giant-chirped pulse width are suitable for the pulse amplification application. Preferably, they can be used as an alternative seed pulse to replace the femtoseconds and picoseconds pulse in the chirped pulse amplification (CPA).

In the early years, several passive SAs have been reported in the literature, including semiconductor saturable absorber mirrors (SESAMs) and a few class of nanomaterials [10]. SESAMs has been proven able to generate a considerably stable short pulsed-laser at a high repetition rate and peak power. However, SESAMs suffers from few drawbacks such as narrow operational bandwidth (< 100 nm), relatively intricate and expensive in fabrication [11], which limits their practical operation. Due to this, alternative SAs have been explored, including carbon nanotubes (CNT) [12,13] and graphene (2D) [14–16]. Additionally, Topological insulators (TIs) [17–19], Transition metal dichalcogenides (TMDs) [20,21] and Black phosphorus (BP) [6,22,23] have also been proposed as alternative SAs. However, these materials are still new, and their performances under real operations have not been fully verified. The CNTs has an operating wavelength which significantly depends on the nanotube's diameter [24], and the existence of CNTs various diameters may lead to extra linear losses. Graphene, for instance, has low optical absorption of 2.3% per layer [25]. The TMD materials have low impurity and uniformity as well as low modulation depth [26,27]. Additionally, the TI materials involve complex fabrication due to the existence of two different elements which suffer from structural instability and high chemical activity [28,29]. BP, on the other hand, is a polarization-dependent and is a hydrophilic material [23] (sensitive to water or humid environment). Thus, integrating BP in the cavity would require an additional protective case. Also, the nanomaterials suffer from low damage threshold and their optical workability is greatly depended on the synthesized material uniformity and impurity. These restrictions have encouraged scientists to explore another novel SAs that able to provide simplicity, cost-efficiency, durability and reliability in both conditions; laser set-up and operation such as metal oxides and fibre SA.

For many years, Holmium, a lanthanide rare-earth element has been widely used as a dopant ion in the fabrication of a Holmium-doped fibre (HDF). The HDF SA had been reported to have a maximal modulation depth of 56% at 1950 nm, and around 37% at both 1930 nm and 1970 nm wavelengths, while the saturation power was measured to be 20 mW at the corresponding wavelengths [30]. In addition to that, the Holmium also is easily found as Holmium oxide (Ho_2O_3) and this material can be dissolved into Polyvinyl alcohol (PVA) solution to fabricate a composite film SA. In earlier works, we demonstrated a Holmium based microseconds pulse, using Holmium oxide PVA film (HOPF) and a segment of HDF as a passive Q-switcher in a Thulium-doped fibre laser (TDFL). The HOPF SA generated a minimum pulse width of 2.57 μs at a central wavelength of 1953 nm. On the other hand, the HDF SA operating at 1972 nm wavelength, produced a minimum pulse width of 2.27 μs. In the aspect of reliability, these Holmium based SAs showed comparable laser performances as the other nanomaterial SAs. However, in terms of durability, the HDF SA offers better thermal damage threshold as compared to the film SAs (including the HOPF SA) since it has a considerably high melting point of silicate glass.

In this paper, we revealed that by integrating an additional length of 10 m long Scandium-doped (Sc-DF) fibre with the Holmium based SAs in the TDFL cavity, nanoseconds pulsed fibre laser operating in the 2-micron regime could be stably generated. Experimentally we obtained a stable nanoseconds pulses train with a pulse width of 57 ns, via the HOPF SA and 53 ns via the HDF SA. We believed that this is the first demonstration thus far, reporting the use of Holmium based SAs in promoting a stable nanoseconds pulse in the TDFL ring cavity.

2. Fabrication and characterization of the holmium based SA

The HOPF SA was fabricated via a drop-casting technique, consisting of a 1:4 (Ho_2O_3: PVA) element ratio, and has a film thickness of ˜50 μm. The detailed of the film SA's fabrication process was explained in our previous work [31]. On the other hand, the HDF SA was obtained from a nano-engineered Holmium doped yttria-alumina-silica glass-based optical preform. The preform was fabricated via the Modified chemical vapour deposition (MCVD) process along with the solution doping technique. The detailed of the HDF synthesis could be found in a previous report [32].

Fig. 1 provides the linear absorption profile of the HDF SA and the HOPF SA measured at the corresponding nanoseconds pulsed laser operating wavelength. As depicted, the HDF SA shows a slightly higher optical absorption of 5.04 dB at 1963 nm wavelength as

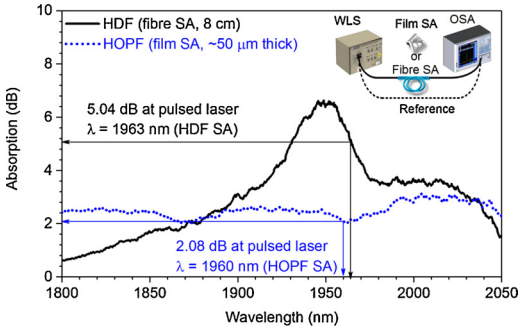

Fig. 1. Linear absorption of the HDF SA and HOPF SA at the respective pulsed laser operating wavelength.

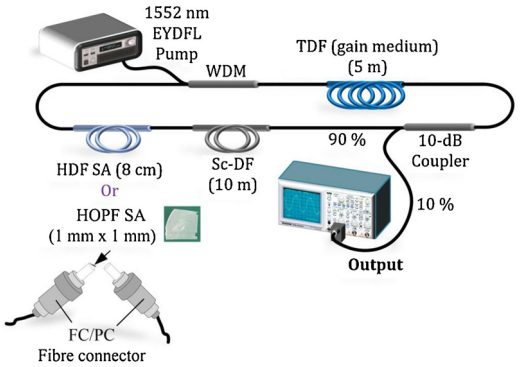

Fig. 2. Schematic diagram of the TDFL ring-cavity configuration.

opposed to the HOPF SA with only 2.08 dB at 1960 nm. The inset of Fig. 1 depicts the linear absorption set-up, comprising a broadband white light source (WLS), the Holmium based SAs and an Optical spectrum analyzer (OSA). Through experiments, the linear absorption from both Holmium SAs was investigated sufficiently of inducing a stable nanoseconds pulse at the 2-micron region.

3. Nanoseconds pulsed fibre laser configuration

The proposed TDFL mode-locked configuration is illustrated in Fig. 2. The ring cavity consists of 1552 nm erbium-ytterbium co-doped fibre laser (EYDFL), 1550/2000 wavelength division multiplexer (WDM), 5 m long Thulium-doped fibre (TDF, Nufern SM-TSF-9/125), 10-dB optical coupler and 10 m Sc-DF. (GVD, β_2 of 60 ps^2/km at 2000 nm). The Sc-DF has a group velocity dispersion (GVD, β_2 of 60 ps^2/km at 2000 nm). The integration of the Sc-DF was to include favourable optical nonlinearity and dispersion in the cavity. The gain medium (TDF) has a numerical aperture (NA) of 0.15, a core/cladding diameter of 9 µm/125 µm and a GVD of 86.8 ps^2/km. The TDF peak core absorptions are at 1180 nm (9.3 dB) and 793 nm (27 dB/m), respectively. The rest of the cavity length was occupied by a normal single-mode fibre (SM-28). The total cavity length was measured to be ˜23.5 m. The 10-dB coupler used in the set-up retained 90% of the laser output to be oscillating inside the TDFL cavity. The rest, 10% of the output was diverted out for various real-time measurements. To promote a self-starting TDFL nanoseconds pulses train, the Holmium based SAs, (either the HDF SA or the HOPF SA) was integrated into the TDFL cavity. The HOPF SA was cut into 1 mm x 1 mm size and sandwiched between two clean fibre ferrules with the aid of index matching gel. The joint was then tightened using a fibre adapter. Meanwhile, the HDF SA was prepared by integrating a segment of 8 cm long HDF in the cavity through a fusion splicing method.

The TDFL nanoseconds pulse optical characteristic was measured via an OSA (Yokogawa AQ6735), while the corresponding pulses train and the frequency domain were examined via a 500 MHz oscilloscope (OSC, LeCroy Wavejet 352A) and a radio frequency spectrum analyzer (RFSA, Anritsu, MS2683A), respectively. Both the oscilloscope and the RFSA were pre-connected with a 7 GHz photodetector (EOT ET-5010 F InGaAs) to allow optical signal interpretations. A combination of a power meter and a thermal sensor was employed to measure the laser output power.

4. Nanoseconds pulsed fibre laser performances

Without any SA in the resonator, a continuous wave (CW) laser centring at 1972 nm was first established at the CW threshold pump power of 235 mW. No pulses train could be detected even with further rises of the pump power. Next, we integrated the 8 cm HDF SA in the resonator, and gradually elevated the pump power. A self-starting 8.51 MHz pulsed laser began to emerge steadily as the pump power rose to 491 mW and remained stable up to the maximum pump power of 656 mW. Beyond this value, the pulsed laser started to diminish into a CW laser.

The temporal performance of the TDFL nanoseconds pulses taken at 491 mW as depicted in Fig. 3(a) has a repetition rate of 8.51 MHz with a corresponding pulse period of 118 ns. The pulse width measured at the full-wave at half maximum (FWHM) is around 53 ns. As seen in the inset of Fig. 3(a), the pulses trace in a wider span shows a considerably stable nanoseconds pulse formation, and without any noticeable pulse instability or interference. The RF spectrum as given in Fig. 3(b) has a fundamental frequency (FF) of 8.51 MHz and a relatively high signal to noise ratio (SNR) of 62 dB, and generally confirms the stability of the generated pulses. Fig. 3(c) shows the optical spectrum of the pulsed laser centring at 1963 nm wavelength with a 3 dB spectral bandwidth (3 dB SB) of 1.3 nm. The durability of the HDF SA was then examined by leaving the fibre SA operated in the cavity at the maximum pump power of 656 mW for nearly 2 h, as depicted in Fig. 3(d). As shown in the figure, the output spectrums taken at different durations, show no significant wavelength shift nor intensity change, suggesting that the pulsed laser operated stably within the test period. This also indicated that the HDF SA was in good condition and operated below the thermal damage threshold temperature. Fig. 3(e) shows the TDFL nanoseconds pulsed laser performances, in relation to the pump power. As illustrated, the output power increases almost linearly from 3.03 mW to 7.41 mW with the rise of pump power from 491 mW to 656 mW. The slope efficiency is calculated as 2.69%. On the other hand, the pulse energy is seen ascending from 0.36 nJ to a maximum of 0.87 nJ.

The HOPF SA was then employed in the TDFL cavity instead of HDF SA, and the pump power was gradually increased. A stable

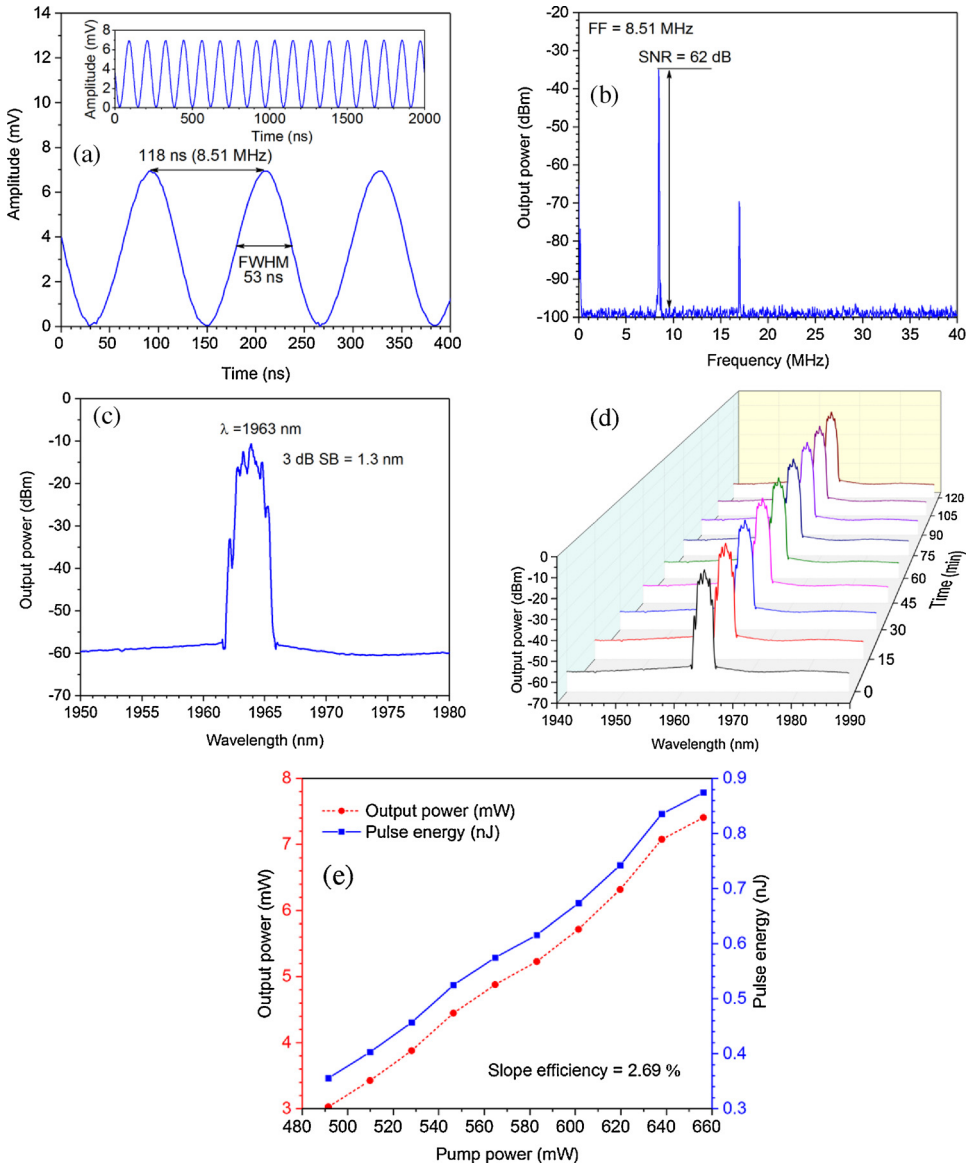

Fig. 3. The performance of the TDFL nanosecond pulses via HDF SA (a) Pulses train with the inset depicting the pulsed-laser in a wider span of 2000 ns, (b) RF spectrum, (c) Output spectrum (d) Output spectra stability (e) Output power and pulse energy as the function of pump power.

nanoseconds pulse with a repetition rate of 8.53 MHz could be stably observed as the pump power hit the threshold of 418 mW. The pulsed laser remained steadily until the pump power reached a maximum of 637 mW. After surpassing the maximum pump power, the pulses collapsed into the CW. The oscilloscope trace of the developed pulse as shown in Fig. 4(a), has a pulse width of 57 ns. The pulse frequency is obtained as 8.53 MHz which is corresponding to a pulse period of 117 ns. The inset of Fig. 4(a) shows the pulses train observed in a broader span, where the generated pulse is seen in a symmetrical shape with its neighbours, suggesting that the nanoseconds pulse is stable. The frequency-domain of the pulsed laser as shown in Fig. 4(b), has an FF of 8.53 MHz and is coherence with the pulse frequency obtained in the time domain (Fig. 4(a)). The SNR of the FF, measured from the peak to the noise floor level is obtained as 51 dB. The pulsed laser has an optical spectrum that peaks at 1960 nm and a 3 dB spectral bandwidth of 2 nm, as illustrated in Fig. 4(c). Fig. 4(d) shows the output spectra stability, observed at a duration of 30 min with a spectrum sampling rate of 5 min. As demonstrated no significant change could be detected on the output spectra central wavelength and output power intensity, indicating that the pulsed laser is stable within the tested duration. Additionally, Fig. 4(e) depicts the output power and pulse energy in relation to the pump power. As shown, the output power ascends from 2.93 mW to 5.29 mW, as the pump power elevated from 418 mW to a maximum of 637 mW. The slope efficiency corresponds to the pump power inclination line is obtained as 1.1%. The pulse energy is seen increasing against the pump power, giving the maximum pulse energy of 0.62 nJ which is obtained at the maximum pump of 637 mW. To inspect the durability of the film SA under a continuous usage, the HOPF SA was left operating in the

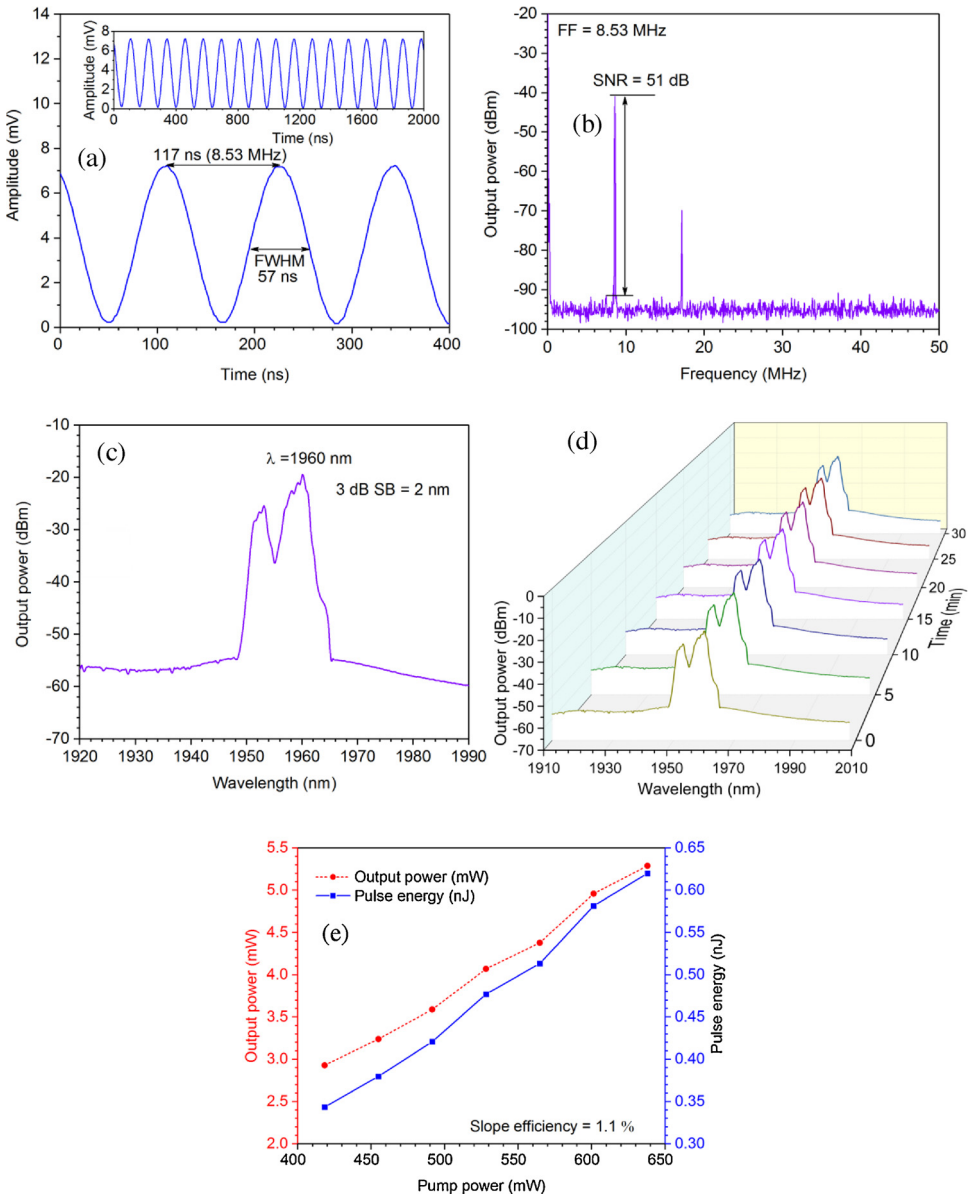

Fig. 4. The performance of the TDFL nanosecond pulses via HOPF SA (a) Pulses train with the inset depicting the pulsed-laser in a wider span of 2000 ns, (b) RF spectrum, (c) Output spectrum (d) Output spectra stability (e) Output power and pulse energy as the function of pump power.

TDFL cavity at the maximum pump power (Fig. 4(d)). The result indicated that the pulses train stably sustained only within 30 min, before losing its pulsed shape. This suggested that the film SA may have melted during the operation.

In these experiments, an additional length of 10 m long Sc-DF was integrated into the experiment to assist the Holmium based SAs in inducing stable self-starting nanoseconds pulsed laser by providing enough dispersion and nonlinearity in the cavity. As to obtain considerably narrow pulse-width, (particularly in the ultra-short pulse regime) both two parameters; dispersion and nonlinearity need to be perfectly balanced. Furthermore, the additional length of the Sc-DF would also improve the pulse energy by slightly broadening the pulse width. The improved pulse energy would be enough to saturate the Holmium SAs at a moderate pump power.

Table 1 compares the TDFL nanoseconds pulse laser performances generated by the HDF SA and the HOPF SA. As shown, the HDF SA generated a longer peak wavelength of 1963 nm, a higher maximum output power of 7.41 mW, greater maximum pulse energy of 0.87 nJ, and a better slope efficiency of 2.69%. However, much higher threshold pump power was needed to induce the HDF based nanoseconds pulsed laser as the light need to be propagated through a longer cavity length as compared to the thin film SA, (HOPF, ~50 μm thickness). As summarized in the table, both SAs generates about the same pulse repetition rate and pulse width, attributed to the same element used as the SA. In overall, the fibre-based SAs was examined capable of handling much longer laser operation at the maximum pump power as they have a considerably higher thermal damage threshold. Apart from that, they also hold the advantage

Table 1
Optical performances comparison between the HDF SA and the HOPF SA.

Optical quantity	Unit	HDF (fibre SA)	HOPF (film SA)
Peak wavelength	nm	1963	1960
Pump power	mW	491-656	418-637
Max. output power	mW	7.41	5.29
Slope efficiency	%	2.69	1.1
Max. pulse energy	nJ	0.87	0.62
Repetition rate	MHz	8.51	8.53
Pulse width	ns	53	57
SNR	dB	62	51
Optical absorption	dB	5.04	2.08

of all fibre structure that easily provides robustness, compactness, maintenance-free and simplicity in the laser set-up [33].

5. Conclusion

We have demonstrated and compared nanoseconds pulsed laser based on Holmium SAs by incorporating 8 cm HDF and ~50 μm HOPF SA in the TDFL. Both SAs were fabricated in-house and showed a sufficient linear absorption in the TDF (gain medium) 2-micron transmission region. The HDF SA with the assistance of 10 m long Sc-DF promoted a nanoseconds pulsed laser, centered at the 1963 nm within a pump power of 491–656 mW. The pulse repetition rate and the pulse width were 8.51 MHz and 53 ns, separately, while the maximum output power and the maximum pulse energy were obtained as 7.41 mW and 0.87 nJ, respectively. On the other hand, the HOPF SA with the help of 10 m long Sc-DF induced a stable nanoseconds pulsed laser operating at 1960 nm wavelength within a pump power of 418–637 mW. The pulsed laser had a repetition rate of 8.53 MHz and a pulse width of 57 ns. The generated maximum output power was 5.29 mW, while the maximum pulse energy was calculated to be 0.62 nJ. These nanoseconds pulsed fibre laser based on the Holmium SAs would offer simplicity, compactness and reliability towards the development of a portable laser source system.

Acknowledgements

M.F.A. Rahman acknowledges the Universiti Teknikal Malaysia Melaka and the Kementerian Pelajaran Malaysia for the financial support given under the SLAB/SLAI award. This work is also supported by the University of Airlangga through Mandate Research Grant (2019).

References

[1] A. El-Sherif, T. King, Soft and hard tissue ablation with short-pulse high peak power and continuous thulium-silica fibre lasers, Lasers Med. Sci. 18 (2003) 139–147.
[2] H.-b. Wei, J. Zhuo, X.-w. Sun, K. Pang, Y. Shao, S.-j. Liang, et al., Safety and efficiency of thulium laser prostate resection for the treatment of benign prostatic hyperplasia in large prostates, Lasers Med. Sci. 29 (2014) 957–963.
[3] I. Mingareev, F. Weirauch, A. Olowinsky, L. Shah, P. Kadwani, M. Richardson, Welding of polymers using a 2 μm thulium fiber laser, Opt. Laser Technol. 44 (2012) 2095–2099.
[4] J. Wang, W. Lu, J. Li, H. Chen, Z. Jiang, J. Wang, et al., Ultrafast thulium-doped fiber laser mode locked by monolayer WSe 2, IEEE J. Sel. Top. Quantum Electron. 24 (2018) 1–6.
[5] J. Wang, X. Liang, G. Hu, Z. Zheng, S. Lin, D. Ouyang, et al., 152 fs nanotube-mode-locked thulium-doped all-fiber laser, Sci. Rep. 6 (2016) 28885.
[6] J. Sotor, G. Sobon, M. Kowalczyk, W. Macherzynski, P. Paletko, K.M. Abramski, Ultrafast thulium-doped fiber laser mode locked with black phosphorus, Opt. Lett. 40 (2015) 3885–3888.
[7] E. Kelleher, J. Travers, Z. Sun, A. Rozhin, A. Ferrari, S. Popov, et al., Nanosecond-pulse fiber lasers mode-locked with nanotubes, Appl. Phys. Lett. 95 (2009) 111108.
[8] H. Xia, H. Li, Z. Wang, Y. Chen, X. Zhang, X. Tang, et al., Nanosecond pulse generation in a graphene mode-locked erbium-doped fiber laser, Opt. Commun. 330 (2014) 147–150.
[9] Y. Zhan, C. Wang, Nanosecond pulse generation in a MoS2 mode-locked ytterbium-doped fiber laser, Opt. Quantum Electron. 48 (2016) 117.
[10] R.I. Woodward, E.J. Kelleher, 2D saturable absorbers for fibre lasers, Appl. Sci. 5 (2015) 1440–1456.
[11] U. Keller, Recent developments in compact ultrafast lasers, Nature 424 (2003) 831–838.
[12] J. Wang, X. Liang, G. Hu, Z. Zheng, S. Lin, D. Ouyang, et al., 152 fs nanotube-mode-locked thulium-doped all-fiber laser, Sci. Rep. 6 (2016).
[13] S.Y. Set, H. Yaguchi, Y. Tanaka, M. Jablonski, Ultrafast fiber pulsed lasers incorporating carbon nanotubes, IEEE J. Sel. Top. Quantum Electron. 10 (2004) 137–146.
[14] J. Liu, J. Xu, P. Wang, Graphene-based passively Q-switched 2μm thulium-doped fiber laser, Opt. Commun. 285 (2012) 5319–5322.
[15] G. Sobon, J. Sotor, I. Pasternak, A. Krajewska, W. Strupinski, K.M. Abramski, Thulium-doped all-fiber laser mode-locked by CVD-graphene/PMMA saturable absorber, Opt. Express 21 (2013) 12797–12802.
[16] Y. Wang, W. Ni, S.Y. Set, S. Yamashita, Mode-locked thulium-doped Fiber laser using a single-layer-graphene-covered tapered fiber, IEEE Photonics Technol. Lett. 29 (2017) 913–916.
[17] M. Jung, J. Lee, J. Koo, J. Park, Y.-W. Song, K. Lee, et al., A femtosecond pulse fiber laser at 1935 nm using a bulk-structured Bi 2 Te 3 topological insulator, Opt. Express 22 (2014) 7865–7874.
[18] J. Lee, M. Jung, J. Koo, C. Chi, J.H. Lee, Passively Q-Switched 1.89-μm fiber laser using a bulk-structured Bi 2 Te 3 topological insulator, IEEE J. Sel. Top. Quantum Electron. 21 (2015) 31–36.
[19] Z. Luo, C. Liu, Y. Huang, D. Wu, J. Wu, H. Xu, et al., Topological-insulator passively Q-Switched double-clad fiber laser at 2 um wavelength, IEEE J. Sel. Top. Quantum Electron. 20 (2014) 1–8.

[20] Z. Luo, Y. Huang, M. Zhong, Y. Li, J. Wu, B. Xu, et al., 1-, 1.5-, and 2-μm fiber lasers Q-switched by a broadband few-layer MoS 2 saturable absorber, J. Light. Technol. 32 (2014) 4077–4084.
[21] J. Wang, W. Lu, J. Li, H. Chen, Z. Jiang, J. Wang, et al., Ultrafast thulium-doped Fiber laser mode locked by monolayer WSe2, IEEE J. Sel. Top. Quantum Electron. (2017).
[22] Y. Chen, G. Jiang, S. Chen, Z. Guo, X. Yu, C. Zhao, et al., Mechanically exfoliated black phosphorus as a new saturable absorber for both Q-switching and mode-locking laser operation, Opt. Express 23 (2015) 12823–12833.
[23] J. Li, H. Luo, B. Zhai, R. Lu, Z. Guo, H. Zhang, et al., Black phosphorus: a two-dimension saturable absorption material for mid-infrared Q-switched and mode-locked fiber lasers, Sci. Rep. 6 (2016) 30361.
[24] S. Yamashita, Y. Inoue, S. Maruyama, Y. Murakami, H. Yaguchi, M. Jablonski, et al., Saturable absorbers incorporating carbon nanotubes directly synthesized onto substrates and fibers and their application to mode-locked fiber lasers, Opt. Lett. 29 (2004) 1581–1583.
[25] Z. Luo, M. Zhou, J. Weng, G. Huang, H. Xu, C. Ye, et al., Graphene-based passively Q-switched dual-wavelength erbium-doped fiber laser, Opt. Lett. 35 (2010) 3709–3711.
[26] B. Chen, X. Zhang, K. Wu, H. Wang, J. Wang, J. Chen, Q-switched fiber laser based on transition metal dichalcogenides MoS 2, MoSe 2, WS 2, and WSe 2, Opt. Express 23 (2015) 26723–26737.
[27] Z. Yu, Y. Song, J. Tian, Z. Dou, H. Guoyu, K. Li, et al., High-repetition-rate Q-switched fiber laser with high quality topological insulator Bi 2 Se 3 film, Opt. Express 22 (2014) 11508–11515.
[28] S. Lu, C. Zhao, Y. Zou, S. Chen, Y. Chen, Y. Li, et al., Third order nonlinear optical property of Bi 2 Se 3, Opt. Express 21 (2013) 2072–2082.
[29] F. Bonaccorso, Z.J.O.M.E. Sun, Solution processing of graphene, topological insulators and other 2d crystals for ultrafast photonics, Opt. Mater. Express 4 (2014) 63–78.
[30] J. Gene, S.K. Kim, S. Do Lim, Validity analysis of holmium-doped fiber as saturable absorber for passively Q-switched thulium-doped fiber laser, J. Light. Technol. 36 (2018) 2183–2187.
[31] M. Rahman, M. Rusdi, M. Lokman, M. Mahyuddin, A. Latiff, A. Rosol, et al., Holmium oxide film as a saturable absorber for 2 μm Q-switched fiber laser, Chinese Phys. Lett. 34 (2017) 054201.
[32] M. Rahman, A. Dhar, S. Das, D. Dutta, M. Paul, M. Rusdi, et al., An 8 cm long holmium-doped fiber saturable absorber for Q-switched fiber laser generation at 2-μm region, Opt. Fiber Technol. 43 (2018) 67–71.
[33] A. Kurkov, E. Sholokhov, O. Medvedkov, All fiber Yb-Ho pulsed laser, Laser Phys. Lett. 6 (2009) 135–138.